Title: **Plant species and plant neighbor identity affect associations between plant assimilated C inputs and soil pores**

H. Zheng[1], A.K. Guber[2,3], Y. Kuzyakov[4,5], W. Zhang[6], and A. N. Kravchenko[2,3]*

[1] Research Institute of Agricultural Resources and Environment, Jilin Academy of Agricultural Science, Changchun, 130033, China

[2] Department of Plant, Soil and Microbial Sciences, Michigan State University, East Lansing, MI, USA

[3] DOE Great Lakes Bioenergy Research Center, Michigan State University, East Lansing, MI, USA

[4] Department of Agricultural Soil Science, University of Göttingen, Göttingen, Germany

[5] RUDN University, Moscow, Russia

[6] College of Geographical Sciences, Inner Mongolia Normal University, Hohhot, 010022, Inner Mongolia, China

*Corresponding author:

Email: kravche1@msu.edu

Keywords: X-ray computed micro-tomography, $^{13}CO_2$ pulse labeling, prairie, switchgrass, big bluestem, wild bergamot, pore-size distribution, soil pore architecture, soil pore structure, plant neighbor identity

Acknowledgements: We would like to thank Jim Muns from MSU Phy/Astronomy Research Shop for building the micro-sampling device. We thank Maxwell Oerther for help with laboratory analysis and Dr. Hasand Gandhi for conducting ^{13}C measurements. Support for this research was provided by the NSF DEB Program (Award # 1904267), by the Great Lakes Bioenergy Research Center, U.S. Department of Energy, Office of Science, Office of Biological and Environmental Research (Award DE-SC0018409), by the National Science Foundation Long-term Ecological Research Program (DEB 1832042) at the Kellogg Biological Station, and by Michigan State University AgBioResearch. YK thanks for the support of the "RUDN University program 5-100".

The μCT scanning was performed at GeoSoilEnviroCARS (The University of Chicago, Sector 13), Advanced Photon Source (APS), Argonne National Laboratory. GeoSoilEnviroCARS is supported by the National Science Foundation - Earth Sciences (EAR - 1634415). This research used resources of the Advanced Photon Source, a U.S. Department of Energy (DOE) Office of Science User Facility operated for the DOE Office of Science by Argonne National Laboratory under Contract No. DE-AC02-06CH11357.

Abstract

Greater plant diversity is known to facilitate soil C gains, yet the exact mechanisms of this effect are still under intensive discussion. Whether a plant grows in monoculture or in a multi-species mixture can affect allocation of plant assimilates, belowground exudation, and microbial stimulation. The goal of this study was to examine the effects of inter-cropping on a previously overlooked aspect of plant-soil interactions, namely, on locations where plant assimilated C is allocated within the soil pore system and its subsequent fate in relation to soil pore size distributions. The soil for the study originated from a greenhouse experiment with switchgrass (*Panicum virgatum* L.) (var. Cave'n'Rock) (SW), big bluestem (*Andropogon gerardii* Vitman) (BB), and wild bergamot (*Monarda fistulosa* L.) (WB) grown in monocultures and in inter-cropped pairs and subjected to species specific ^{13}C pulse labeling (Kravchenko et al., 2021). Intact soil cores (8 mm Ø) were collected from the experimental pots, subjected to a short-term (10 day) incubation, X-ray computed micro-tomography (μCT) scanning, and soil ^{13}C micro-sampling "geo-referenced" to μCT images. Results indicated that in the plant systems with demonstrated interplant C transfer soil ^{13}C was positively correlated with <10 μm Ø pores immediately after plant termination and with 20-80 μm Ø pores after the incubation. In the systems without marked interplant C transfer soil, ^{13}C was positively correlated with 20-30 μm Ø pores, however, the correlations disappeared after the incubation. Soils from the systems with demonstrated belowground C transfer displayed lower losses of root-derived C during incubation than the systems where interplant C transfer was negligible. Factors facilitating interplant C transfer appear to also lead to placement of root-derived C into smaller pores and to its greater protection there.

Introduction

Plants are the primary source of soil organic C, which they supply as dead root biomass, live root rhizodeposits, and root contributions to mycorrhizal and bacterial symbionts (Clemmensen et al., 2013; Kätterer et al., 2011; Pausch and Kuzyakov, 2017). Plant species can differ substantially in terms of the amounts of assimilated C that they transfer belowground (Kuzyakov and Domanski, 2000; Peixoto et al., 2020). Properties of plant C inputs, e.g., C:N ratios or lignin contents, also may differ depending on the species, growth stage, growth conditions, and plant community composition (Sterner and Elser, 2002).

However, there are indications that not only the identity of the plant but also the identity of its neighbors can influence the amounts of plant-derived C inputs and the fate of the inputs (Warembourg et al., 2004). Presence of neighbors evokes belowground plant competition, affecting C inputs via a multitude of pathways. Among those are enhanced investments into root growth, production of chemical exudates to influence competitor roots, and differential stimulation of microbial communities (Callaway et al., 2003).

Assessments of belowground C inputs from plants of different species grown in different plant diversity settings, e.g., monocultures vs. multi-species mixtures, are typically obtained through ^{13}C and ^{14}C plant labeling experiments. With few exceptions (Fan et al., 2008; Rasmussen et al., 2007; Warembourg et al., 2004), such experiments simultaneously label all studied plants. This approach has generated insightful findings regarding overall contributions of multi-species mixtures to new C inputs and their subsequent microbial processing (Dijkstra et al., 2010; Ladygina and Hedlund, 2010; Mortensen et al., 2021). However, it precludes analyses of individual species' inputs and limits assessments of the fate of the photo-assimilated C originated from different plants. The current study originates from a multi-species greenhouse experiment (Kravchenko et al., 2021), where individual members of monocultures and two-species mixtures were selectively ^{13}C labeled. The experiment demonstrated that the interplant belowground C transfer is related to soil enrichment with photo-assimilated C; and that the identity of the neighbors can play a sizeable role in such enrichment (Kravchenko et al., 2021). These results motivated further exploration of the specific mechanisms driving placement and protection of the added photo-assimilated C in multi-species systems.

Contributions of plant-derived C to the long-term soil C storage can be related to where within the soil matrix, that is into pores of what size ranges, it is placed. When new C is placed

into small (Ø few microns) pores it can be better protected because (i) the micro-environmental conditions within the small pores are less favorable to decomposition (Keiluweit et al., 2016), (ii) the small pores are populated by K-strategists (such as *Acidobacteria*) (Negassa et al., 2015) with slower utilization of organic compounds and greater carbon use efficiency (Kravchenko et al., 2020), (iii) there is a greater possibility of a direct contact between organic compounds and soil minerals enabling physico-chemical binding and protection (Kravchenko et al., 2019), and (iv) much lower accessibility of new C for decomposers and their enzymes (Pagel et al., 2020; Portell et al., 2018). On the contrary, when new C is placed into medium (Ø few tens of microns) pores it can be readily available to microbial decomposers triggering greater losses (Killham et al., 1993; Ruamps et al., 2011; Strong et al., 2004). Plant assimilated C inputs from cereal rye (*Secale cereale* L.) were positively associated with medium pores likely accessible to fine roots and root hairs (Negassa et al., 2015; Quigley et al., 2018). Yet, the associations became negative after the incubation, suggesting that greater losses of new C also took place within these pores. Quigley with colleagues (Quigley et al., 2018) referred to greater inputs of plant assimilated C into medium pores, subsequently followed by quick decomposition there, as "easy come easy go" phenomenon. However, this phenomenon has only been studied in cereal rye (Quigley et al., 2018) – the crop strongly modified by agricultural selection – and, to our best knowledge, not explored in any other plant species. Here we explore whether the placement of plant assimilated C and its subsequent fate is related to pores of different sizes in natural plant communities, grown in monoculture or intercropped.

Spatial distribution of soil C at fine scales can be highly variable due to variability in rhizodeposition and activities of microbial decomposers (Nunan et al., 2006; Nunan et al., 2003; Pausch and Kuzyakov, 2011). The hotspot nature of microbial activity carries important implications for understanding soil C cycling (Kuzyakov and Blagodatskaya, 2015). However, most experiments exploring plant-assimilated C inputs have been based on analyses of well mixed and homogenized soil – a practice that maximizes accuracy and efficiency in experimental treatment comparisons but precludes assessments of small-scale spatial patterns. A number of recent advanced tools for visualization and quantification of spatial patterns of plant C inputs have been successfully implemented, including nanoscale secondary ion mass spectrometry (NanoSIMS) (Mueller et al., 2013; Vidal et al., 2018), ^{14}C phosphor imaging (Holz et al., 2018; Pausch and Kuzyakov, 2011), and laser ablation-isotope ratio mass spectrometry (LA-IRMS)

(Denis et al., 2019). However, at present all these methods of fine scale soil C mapping rely on advanced technology and equipment, out of reach for majority of soil researchers. Here we assess spatial variability patterns in soil C at mm-scale using an inexpensive, yet reliable, technique of site-specific micro-sampling.

We hypothesize that the location where the new plant-derived C is placed depends both on the identity of the plant and on the identities of the plant's neighbors. Here, by "location" we refer to soil pores of a specific size range. We also hypothesize that the location of its placement affects whether the new plant-derived C is protected within the soil matrix or lost as CO_2. The specific objectives of the study were to assess the role of the plant species identity and the identity of its neighbors in defining 1) localization patterns of plant-assimilated C additions within the soil matrix, 2) associations between root-derived C and fractions of pores of different sizes, and 3) changes in the associations between root-derived C and pores developing during a 10-day incubation – the period common for microbial turnover in the rhizosphere.

Methods

Overview of the greenhouse experiment

A detailed description of the greenhouse experiment which generated soil samples for this study is provided in Kravchenko et al. (2021). Here we just briefly present its key components. The soil for the experiment was collected at 0-10 cm depth from an agricultural field at W. Kellogg Biological Station in Southwest Michigan, USA. The soil is a sandy loam Alfisol of Kalamazoo series, with soil organic C of 7.5 g/kg and pH of 5.7. The soil was ground to pass a 2 mm sieve, thus had its existing pore architecture largely destroyed, in order to facilitate detection of new pore architecture formation in response to the new plant growth. Sieved soil was uniformly packed into ~10×10×10 cm^3 pots to achieve a bulk density of ~1.1 g cm^{-3}.

The three studied plant species were switchgrass (*Panicum virgatum* L.) (var. Cave'n'Rock) (SW), big bluestem (*Andropogon gerardii* Vitman) (BB), and wild bergamot (*Monarda fistulosa* L.) (WB). Two plants were grown per each side of the pot. Planting was conducted either as monoculture, i.e., both sides of each pot were occupied by the plants of the same species, or as intercropped mixtures, i.e., two species per plot, one on each side. The experiment consisted of 50 pots representing 5 replicates of each of 10 experimental plant

154 systems: monocultures of each of the three species (SW, BB, WB); every pair of the two species
155 where only one member of the pair was ^{13}C labeled (e.g., a BB-WB mixture where BB was ^{13}C
156 labeled and WB was unlabeled and a WB-BB mixture where BB was unlabeled and WB was
157 labeled); and an unplanted control soil.
158 ^{13}C pulse labeling (one 6-hr pulse per week for 3 weeks) started when the plants were 2-
159 month-old. For that we used 98% ^{13}C enriched $NaH^{13}CO_3$ solution (equivalent to 88 mg ^{13}C
160 released per pulse event per chamber). H_2SO_4 solution was added in excess to react with all
161 $NaH^{13}CO_3$ to produce $^{13}CO_2$ for plant assimilation. Prior to each labeling, the plants on one side
162 of each pot were tightly covered with a light-impenetrable cover which was kept for the entire
163 duration of the labeling event. Thus, only the plants on one side of the pot could photo assimilate
164 ^{13}C, while the plants on the other side remained unlabeled. The total growing period for the
165 studied plants was 3 months. Root bounding was observed at the bottom of the pots at plant
166 termination; however, it did not affect the top portions of the pots that were subjected to soil
167 sampling (Appendix Fig. 1).
168 Analysis of root ^{13}C abundance after plant termination led to separation of the plant
169 systems into two groups (Kravchenko et al., 2021): 1) the group where substantial amounts of
170 ^{13}C assimilated by the labeled plant were subsequently found in the roots of the unlabeled
171 neighbors and 2) the group where no or negligible amounts of ^{13}C from the labeled plants were
172 found in the unlabeled neighbor plants. The first group consisted of the following plant systems:
173 (source-neighbor) SW-WB, SW-BB, BB-WB, and BB-BB; and will be referred to as the group
174 with C transfer. The second group consisted of the plant systems (source-neighbor): WB-WB,
175 WB-BB, WB-SW, BB-SW, SW-SW; and will be referred to as the group without C transfer. In
176 essence, the ^{13}C transfer was negligible when SW was the unlabeled neighbor and when WB was
177 the labeled source.
178 An outline of the experimental approach used in this study is presented on Fig. 1a. After
179 the greenhouse experiment, the intact cores were collected from the experimental pots. Half of
180 the cores was subjected to μCT scanning, while the other half was first incubated and then μCT
181 scanned. The micro-samples for soil ^{13}C were taken from all scanned cores, and the μCT images
182 were used to generate pore-size distribution data and to identify root and particulate organic
183 matter fragments within the samples. Correlation and regression analyses were implemented to

explore associations between the soil ^{13}C signatures and the volumes of pores of different sizes in non-incubated and post-incubated cores of the studied plant systems.

Soil core sampling and incubation

A total of 60 intact soil cores (Ø 0.8 cm and ~2 cm height) were taken from the labeled sides of the pots from 0.5-2.5 cm depth for subsequent incubation and μCT image analysis (Appendix Fig. 2). The cores were collected into plastic cylinders placed within a mini-push probe. The push probe had a sharp edge and a lip for holding the plastic cylinder to reduce soil compaction when collecting the cores.

We used 30 cores (one core per pot from 3 replicated pots of each treatment) collected immediately after plant termination for μCT scanning and for ^{13}C soil micro-sampling; these will be referred to as non-incubated soil cores. Another 30 cores (one core per pot from 3 replicated pots of each treatment) were subjected to a 10-day incubation followed by μCT scanning and ^{13}C soil micro-sampling; these will be referred to as post-incubation soil cores. The first set of cores provided information on initial spatial patterns of recently added plant-derived C, while the second set of cores provided information on its losses and redistribution. Since it was important to use only the cores that were as intact as possible for subsequent pore analyses via μCT, only a portion of the non- and post-incubation cores originated from the same pot. Therefore, the number of pots containing both a non- and a post-incubation core varied from 1 to 3 per treatment.

For the incubation, the cores were moistened to 50% water filled pore space and placed within 480 ml Mason jars holding a small container with water to reduce evaporation. The incubation was conducted in the dark at 22 °C for 10 days.

It should be noted that while the data from the greenhouse experiment and from the intact cores have been presented in Kravchenko et al (2021), the micro-sampling study reported here consists of an independent set of results representing fine spatial scale.

Soil pore characterization with μCT

A detailed description of the μCT scanning is provided in Kravchenko et al (2021) who also reported pore-size distribution data from non-incubated cores. Here we report the results on

214 the changes in pore-size distributions that took place during the incubation and explore
215 associations between pore-size distributions and soil ^{13}C.
216 In brief, the cores were scanned on the bending magnet beam line, station 13-BM-D of
217 the GeoSoilEnviroCARS at the Advanced Photon Source, Argonne National Laboratory. The
218 scanning energy was 24 keV, and the scanning resolution was 5.6 µm. Prior to µCT scanning
219 both non-incubated and post-incubation cores were air-dried. The µCT image analyses were
220 conducted using ImageJ/Fiji (Rasband, 1997-2015; Schindelin et al., 2012). Image segmentation
221 into solids and pores was conducted using Renyi Entropy segmentation procedure available in
222 ImageJ (Kapur et al., 1985). Roots and fragments of particulate organic matter within the cores
223 were thresholded using the approach described in Kravchenko et al. (2021). Separation of pores
224 into size classes was conducted using the continuous 3D pore-size distribution determination
225 approach of maximally inscribable spheres implemented in Xlib plugin for ImageJ (Munch and
226 Holzer, 2008). The smallest pore size considered in the study had a radius equal to the image
227 resolution, i.e., 5.6 µm. However, it should be noted that visualization of objects, say pores, that
228 are not 2-5 times larger than the image resolution is uncertain (Koestel et al., 2018; Vogel et al.,
229 2010). Thus, the volumes of pores with radii 5.6-17 µm obtained in this study are likely
230 somewhat underestimated.
231
232 *Micro-sampling*
233 The micro-sampling process is illustrated on Fig. 1b. For micro-sampling an intact core
234 (1) was fixed within a sampling table (2). Since the cores were air-dried for the µCT scanning,
235 that is, prior to micro-sampling, DI water (2 ml) was added with a pipette to the surface of the
236 core to facilitate sample collection. Then, a very top layer (1.5 mm) was removed from the soil
237 core and discarded since soil in it could have been affected during core handling and storage. For
238 that, a metal circle with an inner diameter identical to that of the core (Ø 0.8 cm) and with 1.5
239 mm height was placed on top of the core. The soil was gently pushed out of the plastic cylinder
240 of the core to fill the circle using a plunger, and the top 1.5 mm soil layer was removed with a
241 sharp knife using the circle as a guide (3). Then, the procedure was repeated to procure the
242 portion of the core for the actual sampling, but now using a circle with 5 mm height. The
243 resultant 5 mm tall portion of the core was subjected to soil sampling using a mini-sampler that
244 consisted of a set of 5 metal tubes (Ø 2 mm and 5 mm height) mounted on a holder (4). The

sampler was aligned with the 5 mm core portion and pushed into it (5), producing 5 soil micro-samples at specific positions within the soil core that later were matched with the μCT images (Fig. 1b). Each sample tube had a vertical line etched into its side (1), clearly visible on the CT scans; the line was aligned with the line on the mini-sampler when positioning it prior to sampling. Then, the samples were pushed out of the tubes into five pre-weighted tin foil containers (6). The positions of the sampling tubes within the 3D image of the sample were determined after aligning the image of the mini-sampler with the μCT image (Fig. 1c).

The tins with the soil were wrapped, weighted, and subjected to $\delta^{13}C$ soil analysis (7). Prior to wrapping the soil, each tin was carefully examined and visible remains of plant roots or particulate organic matter were removed with tweezers. The full removal of the root residue can never be fully guaranteed. However, the obtained soil micro-samples did not exhibit an association between the volumes of roots and particular organic matter fragments, identified within each micro-sample from μCT images (Fig.1c), and soil $\delta^{13}C$ signatures (Appendix Fig. 3).

The $\delta^{13}C$ analyses were conducted on an elemental analyzer (Vario ISOTOPE CUBE, Elementar) coupled to an isotope ratio mass spectrometer (Isoprime Vision, Elementar). The ^{13}C enrichment data are reported as $\delta^{13}C$ (‰) based on the PeeDee Belemnite standard.

Unfortunately, due to sample mislabeling only 14 (out of 30) of the non-incubated cores could be used for the analysis of the associations between ^{13}C and pores in the non-incubated cores.

Statistical analysis

The data from non-incubated and post-incubation cores were analyzed separately. Depending on the specific research question, the statistical models used in the data analyses consisted of the fixed effect of either plant system treatments, or the plant system treatments combined into C source and non-labeled neighbor groups, or into groups with and without C transfer. All models included the random effect of the soil core nested within either plant system or the respective group variables and used as an error term for testing their effects. Comparisons among the group means were conducted using t-tests, when the respective F-tests for the groups were statistically significant. Data analyses were conducted using PROC MIXED procedure of SAS (SAS 9.4).

Assumptions of normality of the residuals and homogeneity of variances were assessed using normal probability plots and side-by-side box plots, respectively. The assumptions were violated for soil $\delta^{13}C$ data from the micro-samples, which were highly variable with a number of extreme outliers. Thus, we used natural log transformation applied to $\delta^{13}C$ data with added value of 26 – as needed to eliminate negative values prior to transformation.

Associations between volumes of pores of different size groups and soil $\delta^{13}C$ were assessed using Pearson correlation and linear regression analyses (PROC CORR and PROC REG of SAS) separately for non-incubated and post-incubated data sets and by either individual C source/non-labeled neighbor groups or by C transfer groups. Due to extremely high variability of the micro-sample data, we report both the data significant at 0.05 and 0.1 levels, and also mention numeric trends that were consistent with the ad-hoc hypotheses.

Results

Plant assimilated C in soil before and after incubation

Prior to the incubation, the $\delta^{13}C$ signatures in the micro-samples did not significantly differ among the labeled, i.e., C source, plant species (Fig. 2a and Table 1), that is, among the plants in immediate vicinity of which the samples were collected (Appendix Fig. 2). After the incubation, the samples from the soil cores with WB as the C source plant (WB-source) had higher $\delta^{13}C$ than the samples from BB-source and SW-source plant systems (Fig. 2b and Table 1). Identity of the neighbor plant, that is the plant that shared the box with the labeled plant but was not ^{13}C labeled itself, affected the soil $\delta^{13}C$ signature both in the non-incubated and post-incubation cores. Soil $\delta^{13}C$ signatures increased in the order of the neighbor plants SW<BB<WB (Table 1).

For BB- and SW-source systems only, soil of the systems with demonstrated presence of interplant C transfers (systems source-neighbor SW-BB, SW-WB, BB-BB, BB-WB) had higher $\delta^{13}C$, than the systems where the evidence of C transfer was negligible (systems source-neighbor BB-SW, SW-SW) (Appendix Fig. 4). The result was consistently observed in both non-incubated and post-incubation cores ($p<0.05$).

When the entire set of $\delta^{13}C$ measurements across all pots and soil cores was analyzed, the $\delta^{13}C$ change in soil during the incubation was negligible for most plant systems, with the

exception of monoculture SW (SW-SW) (Fig. 2a and 2b). In monoculture SW soil $\delta^{13}C$ decreased from -8 to -17‰ ($p<0.1$). However, when we analyzed the differences between post-incubation and non-incubated cores collected from within the same pots, the ^{13}C losses during the incubation were greater in the systems without interplant C transfer (source-neighbor: WB-WB, WB-BB, WB-SW, BB-SW, SW-SW) than in the systems with C transfer (source-neighbor: SW-WB, SW-BB, BB-WB, and BB-BB) (Fig. 3b). Neither the source plant identity nor the non-labeled neighbor plant identity significantly affected $\delta^{13}C$ changes during incubation (Fig. 3a).

Micro-scale variability of $\delta^{13}C$ within individual soil cores was very high (Fig. 4) and greatly exceeded variability among the individual plant pots and plant systems (Table 2). The variability among the micro-samples from non-incubated cores was more than twice the variability in the micro-samples from post-incubation cores ($p<0.05$).

Pore-size distributions before and after incubation

When examined in individual plant systems, the image-based soil porosity (pores with radii >5.6 μm) of non-incubated cores was not significantly different from that in the post-incubation cores (Table 3). However, in the plant systems with C transfer the image-based porosity of post-incubation cores was higher than that in the non-incubated cores ($p<0.05$).

Across all studied plant systems, the incubation significantly changed pore-size distributions (Fig. 5). The volumes occupied by the smallest pores (5.6-11 μm radius) markedly increased after incubation - the trend consistently observed in all plant systems. On the contrary, the volumes of pores in ~20-100 μm range tended to be higher in the non-incubated than in post-incubation cores. This trend was most pronounced in the plant systems with BB-source and was weaker in SW- and WB-source systems (Fig. 5a). In the plant systems with C transfer the non- vs. post-incubation differences in pores of this size range were negligible, while in the systems without C transfer the differences in pores of this size range were significant ($p<0.05$) (Fig. 5b). There were no consistent differences between non-incubated and post-incubation cores in the volumes of the largest (>100 μm radius) pores.

Associations between plant assimilated C and pores before and after incubation

Associations between volumes of differently sized pores and soil $\delta^{13}C$ differed among the source plants (Fig. 6). Prior to incubation, the higher ^{13}C enrichment corresponded to greater

volumes of the medium sized pores (~11-50 μm radii) in soil from WB-source systems (Fig. 6a). There were only weak (p<0.1) negative correlations between medium sized pores and $\delta^{13}C$ in BB-source systems. It was not possible to reliably assess the correlations in SW plants due to low number of observations (n=10).

After incubation, the correlations between medium sized pores and $\delta^{13}C$ in soil from the plant systems with WB-sources became negative or non-significant, while in BB and, especially, SW-sources positive correlations were observed (Fig. 6b). Examples of correlations between $\delta^{13}C$ and 25 μm radius pores non- and post-incubation in SW- and WB-source samples are shown on Figs. 6e and 6f, respectively.

In the plant systems without C transfer soil $\delta^{13}C$ was weakly (p<0.1) positively correlated with ~20-30 μm radius pores (Fig. 6c); but these correlations were absent in the post-incubation cores (Fig. 6d), yet there were positive correlations with ~60-70 μm pores. In the non-incubated cores from the plant systems with C transfer significant positive correlation was only observed between soil $\delta^{13}C$ and the smallest pores (Fig. 6c); in the post incubation cores soil $\delta^{13}C$ was positively correlated with pores in ~11-40 μm radius range (Fig. 6d).

Discussion

Micro-scale variability of plant C allocation to the soil

Soil matrix affected by growing plants consisted of a complex mosaic of regions with very high levels of new C inputs bordering the regions completely devoid of the new C (Fig. 4). The sharp drops in $\delta^{13}C$ among adjacent soil micro-samples took place within 1-3 mm distances. These distances are consistent with 1-2 mm distances from the roots at which the levels of plant assimilated C tend to decrease to the natural background levels (Denis et al., 2019; Kuzyakov and Razavi, 2019; Pausch and Kuzyakov, 2011; Pausch and Kuzyakov, 2018). The micro-samples from the immediate vicinity of the roots were likely the ones highly enriched in new C as compared to those that contained non-rhizosphere soil.

Importantly, the micro-sample variability dropped after the incubation (Table 2). This drop reflects fast decomposition of new C by microorganisms, which can lead to substantial C losses even during short incubation times (Kuzyakov and Domanski, 2000; Marx et al., 2007).

It should be noted that spatial variability of old soil C, i.e., soil organic matter, at fine spatial scales (Gutierrez-Castorena et al., 2018; Lucas et al., 2020) can be just as high as that of the new C inputs observed in this study. For example, coefficients of variation for soil total organic C within 5 mm Ø macro-aggregates were as high as ~70-100% (Ananyeva et al., 2013).

Root-derived C in soil: differences among species

The identity of the ^{13}C source plant influenced soil $\delta^{13}C$ (Fig. 2). When comparing the three studied ^{13}C sources across all non-labeled neighbors the trend of WB>SW>BB in soil $\delta^{13}C$ was present both prior to incubation (numeric) and after the incubation ($p<0.05$) (Table 2). The amounts of C allocated to the roots and placed into the soil via rhizodeposition can vary substantially among the plant species (see (Pausch and Kuzyakov, 2018) for the latest review). Moreover, the differences among individual species within the same functional group, e.g., within grasses, can be as large as the differences among the groups, e.g., grasses vs. forbs/legumes (Sanaullah et al., 2012). Among the three studied species WB was the plant with the greatest ^{13}C allocations to roots. Average root $\delta^{13}C$ in monoculture WB exceeded 1000‰, while average $\delta^{13}C$ signatures in roots of all other studied systems were less than 700‰ (Kravchenko et al., 2021). This suggests that high ^{13}C allocations to roots by WB is the main reason for higher soil $\delta^{13}C$ under the plant systems with WB ^{13}C source.

However, the identity of the neighbors had as large or even larger effect on the amount of plant assimilated C found in the soil as the identity of the source plant itself. In the plant systems, where WB was a non-labeled neighbor, soil had consistently higher $\delta^{13}C$, regardless of the identity of the C source plant – be it either BB, SW, or WB itself (Table 2). The effect of plant neighbor identity on new C allocations to roots and soil has been reported before. Specifically, Warembourg et al (2004) observed that clover (*Trifolium angustifolium* L.) had a lower proportion of new photo-assimilated C in its roots and a higher proportion in soil when its neighbor was grass *Bromus madritensis* L., than when it was grown with neighbors of its own species. Yet, when *B. madritensis* was the C source plant the proportions of new photo-assimilated C in roots and soil were similar regardless of the identity of the non-labeled neighbor. A number of other factors influencing additions of assimilated ^{13}C to the soil have been studied extensively, including plant development stage (Hupe et al., 2018; Wichern et al., 2007a; Wichern et al., 2007b), plant growth conditions in terms of water, light, and N availability

(Cheng et al., 2003; Pausch et al., 2013; Sanaullah et al., 2012), and symbiosis with arbuscular mycorrhizal fungi (AMF) (Ladygina and Hedlund, 2010). However, the role of and the mechanisms behind the neighbor identity effects have been mostly overlooked and our work is one of the few that bring attention to this potentially sizeable driver of soil C enrichment.

Quantities of plant assimilated ^{13}C lost from the soil during the first few days after plant termination (10-day incubation) tended to be higher in two of the studied monocultures, SW and WB, and lower in their mixtures (Figs. 2 and 3). Tendencies of greater losses of new plant assimilated C from soils of monocultures than of plant mixtures were observed before (Dijkstra et al., 2010; Pausch et al., 2013) and were explained by enhanced plant-microbial competition in plant mixtures due to more intensive N and water use, which can reduce microbial activity (Dijkstra et al., 2010). This notion was further supported by substantially lower activities of extracellular enzymes (Sanaullah et al., 2011) and lower N mineralization rates (De Notaris et al., 2020) in mixtures as compared to monocultures. The lower losses of added C from SW mixtures than from SW monoculture, observed in this study, are also consistent with long-term field results. Namely, field experiments on the studied soil (sandy loam Alfisol of Kalamazoo and Oshtemo series) comparing SW monoculture with diverse plant communities (e.g., native succession vegetation and restored prairie) demonstrated that diverse communities facilitated faster and larger soil C gains (Kravchenko et al., 2019; Sprunger and Robertson, 2018). Greater losses of newly added plant C from the soil in monoculture SW observed here is one potential contributor to lower soil C gains observed in the field.

Root-derived C in soil: associations with soil pores

Associations between soil ^{13}C and pores offer possible explanations for the observed species and neighbor identity effects in terms of new C additions and losses from the soil. The WB source plants generated positive associations between new C with medium sized pores (20-60 μm radius) (Fig. 6a), while BB source plants with small (5.6 μm radius) pores (Fig. 6a). Positive associations between new C with medium sized pores (20-60 μm radius) were observed in the systems with no C transfer (Fig. 6c), while positive associations with small (5.6 μm radius) pores in the systems with C transfer (Fig. 6c). These findings support the notion that different plant species and plant communities with/without C transfer might be placing new C into pores of different sizes.

We propose the following hypothesis on the origin of these results. In the first case, i.e., positive associations with medium pores, the new C was preferentially added into the soil via decomposing roots, via rhizodeposits, and via exudates diffusing from the roots into the rhizosphere. While in the second case, i.e., positive associations with small pores, the C was added via AMF hyphae, which traveled from the roots, through rhizosphere, and into the bulk (non-rhizosphere) soil. Carbon arriving into the soil directly from the roots must necessarily be associated with larger pores than that arriving via AMF, because roots are of greater diameter and populate larger pores than fungal mycelia.

Inter-plant transfer of C and N can take place via direct root contact or via fungal networks. The importance of direct root contact cannot be overlooked (Hupe et al., 2021), yet a substantial portion of new C is often found to transfer among plants via hyphal networks (Montesinos-Navarro et al., 2017; Simard et al., 2012; Simard et al., 1997). It is possible that the positive correlation between soil ^{13}C and small pores in the combined data from all plant systems with C transfer (Fig. 6c) reflect such movement of new C through smaller pores as/via fungal mycelia. While ecological significance of interplant C transfer is still debated (Pfeffer et al., 2004; Robinson and Fitter, 1999; Simard et al., 1997), sizeable involvement of fungi, both AMF and ectomycorrhizal, has been well demonstrated. Small pores are accessible to fungi, since hyphae range in diameters from 2 to 20 μm (Smith and Smith, 2011). A portion of the plant C from fungal networks that does not reach the neighbor plants is transferred to bacteria associated with the hyphae (Vidal et al., 2018) or remains in the hyphae and relatively quickly decomposes upon hyphae death (De Deyn et al., 2011; Johnson et al., 2002). Thus, a substantial amount of plant-derived C within fungal mycelia can be lost into the soil upon fungal death and decomposition. In the systems without C transfer new C was preferentially placed within medium sized pores via root-related routes, generating positive correlations of soil ^{13}C with medium sized pores (Fig. 6c).

Where the C was placed, i.e., either within small or within medium sized pores, defined how well it was protected. Medium sized pores are locations of the greatest microbial activities (Killham et al., 1993; Quigley et al., 2018; Ruamps et al., 2013; Strong et al., 2004) because of good O_2 supply, and consequently are populated by r-strategy organisms with lower C use efficiencies, fast metabolism, and rapid microbial turnover (Kravchenko et al., 2020). New C inputs placed into such pores are quickly processed with substantial amounts subsequently lost as

460 CO_2 (Kravchenko et al., 2020; Quigley et al., 2018) (Fig. 3b and 6d). The C placed into small
461 pores experiences a somewhat different fate. While a substantial portion of it is lost to
462 atmosphere as CO_2, some of the resultant microbially processed C of plant origin is readily
463 associated with soil minerals becoming protected from further decomposition (Vidal et al.,
464 2018). Such associations are easier to achieve in small pores due to closer proximity between soil
465 minerals and new C inputs. Moreover, small pores offer less auspicious environments for
466 microbial activities (Keiluweit et al., 2016; Keiluweit et al., 2017) and are likely populated by K-
467 strategist microorganisms with lower and slower losses of the processed organic as CO_2
468 (Kravchenko et al., 2020). As a result, we observed lower losses of plant C in the soil cores from
469 the plant systems with demonstrated C transfer (Fig. 3b).
470 The associations between pores of specific sizes and plant-derived C in the soil with WB-
471 sources and in the systems without C transfer were consistent with the "easy come easy go"
472 hypothesis of Quigley et al. (2018). In the non-incubated cores, higher soil $\delta^{13}C$ was associated
473 with greater presence of medium-sized pores, while an opposite trend was observed post-
474 incubation (Fig. 6). However, in the soil with BB-sources and in the systems with demonstrated
475 C transfer the soil $\delta^{13}C$ was positively associated with medium pores in the post-incubated cores
476 – an opposite of what was hypothesized (Fig. 6). At this point we do not have an explanation of
477 this result.
478
479 **Conclusions**
480 Beside plant identity, the identity of its neighbors influenced how much of assimilated C
481 was placed in the soil, how it was associated with soil pores, and how well protected it was from
482 subsequent decomposition. In the systems with interplant C transfer the ^{13}C from labeled plants
483 increased with the volume of small pores, while in the systems without interplant C transfer –
484 with the volume of medium pores. These differences prompted a hypothesis on dissimilarities in
485 the mechanisms of adding photo assimilated C to the soil: via mycorrhizal hyphae into small
486 sized pores vs. via roots into medium sized pores. In the latter case the plant-derived C is quickly
487 lost during subsequent incubation. Our findings suggest that greater losses of plant assimilated C
488 from the soil often reported during comparisons of monocultures with inter-cropped plant
489 mixtures are related not only to monoculture vs. polyculture dichotomy, but to the route of plant
490 C additions to the soil and its localization within the soil pores. The plant systems with interplant

491 transfer of assimilated C, both intra- and inter-species tended to lose less C; while somewhat
492 higher losses were observed in the systems where interplant C transfer was negligible.
493
494

Data availability statements

The datasets generated during and/or analyzed during the current study are available from the corresponding author on reasonable request.

Conflict of interest statements

The authors have no relevant financial or non-financial interests to disclose.
The authors have no conflicts of interest to declare that are relevant to the content of this article.
All authors certify that they have no affiliations with or involvement in any organization or entity with any financial interest or non-financial interest in the subject matter or materials discussed in this manuscript.
The authors have no financial or proprietary interests in any material discussed in this article.

Table 1. Soil $\delta^{13}C$ signatures (‰) in the micro-samples taken from the intact cores that were not subjected to the incubation and from the cores subjected to a 10-day incubation. Shown are marginal means of the source plants averaged across all neighbors and marginal means of neighbor plants averaged across all sources with standard errors in parentheses. The letters within each row mark significant differences among the respective source or recipient marginal means ($p<0.1$). The statistical analyses represented by the letters were conducted on log-transformed data (natural log of ($\delta^{13}C$ +26)).

Studied factor	Incubation	Big bluestem	Switchgrass	Wild bergamot
Source (source plants across all neighbors)	not incubated	24.1 (20.8)	11.2 (18.9)	51.9 (20.5)
	incubated	-3.8 (15.2) a	6.3 (14.4) a	37.3 (14.4) b
Neighbor (neighbor plants across all sources)	not incubated	25.8 (16.5) ab	7.3 (20.3) a	54.0 (22.9) b
	incubated	19.7 (13.8) b	-5.7 (15.5) a	25.8 (14.9) b

Table 2. Variances in soil $\delta^{13}C$ signature data at the levels of the plant systems, individual pots and micro-samples before and after the incubation. ** mark the case were the non- and post-incubation variances were significantly different from each other ($p<0.05$).

Source of variation	Non-incubated cores	Post-incubation cores
plant systems	39	51
pots	1306	1041
micro-samples	5216	2340**

528 **Table 3.** Image based porosity (pores with radii >5.6 μm) in the studied plant systems (part 1)
529 and carbon transfer groups (part b). Image based porosity is calculated as percent of the pore
530 voxels in 3D μCT images of the total number of voxels. Shown are the means and standard
531 errors in parentheses. In the top part of the table the low case letters mark differences among the
532 recipient plants within the same source plant incubation treatment (p<0.1); and upper-case letters
533 mark significant differences among the source plants within the same recipient plant and
534 incubation treatment (p<0.1). In the bottom part of the table, the bold low case letters mark
535 significant difference between the non-incubated and post-incubation samples (p<0.05).
536

	Image-based porosity, %					
a)	**Non-incubated cores**			**Post-incubation cores**		
Source plant	**Recipient plant**					
	BB	**SW**	**WB**	**BB**	**SW**	**WB**
BB	7.9 (1.4)	9.3 (1.4)A	8.0 (1.7)	10.8 (1.4)	8.5 (1.7)	9.3 (1.4)
SW	9.1 (1.7)a	13.6 (1.7)bB	8.7 (1.4)a	11.4 (1.4)	9.9 (1.4)	11.6 (1.4)
WB	11.1 (1.4)	7.7 (1.7)A	10.1 (1.4)	10.0 (1.4)	10.1 (1.4)	10.6 (1.4)
b)	**Non-incubated cores**			**Post-incubation cores**		
C transfer group						
Yes	8.4 (0.7)**a**			10.8 (0.7)**b**		
No	10.3 (0.6)			9.9 (0.6)		

537
538

Figure 1. Experiment description and illustration: (a) Outline of the experimental approach. (b) Illustration of the steps of the micro-sampling process, including positioning of the core (1) within the sampling table (2) and cutting off the top 1.5 mm soil layer (3). Then a sampling device is positioned on the core and micro-samples are taken (4 and 5), with soil from the sampling tubes pushed into foil tins (6) for subsequent soil total C and $\delta^{13}C$ analyses (7). (c) A sample µCT image of the portion of an incubated core with yellow circles marking the locations of the micro-samples (left) with the same image with segmented plant roots and fragments of particulate organic matter (green) (center), and a 3D view of a soil core showing pores identified on µCT image (green) and locations of the micro-samples within the core (white) (right).

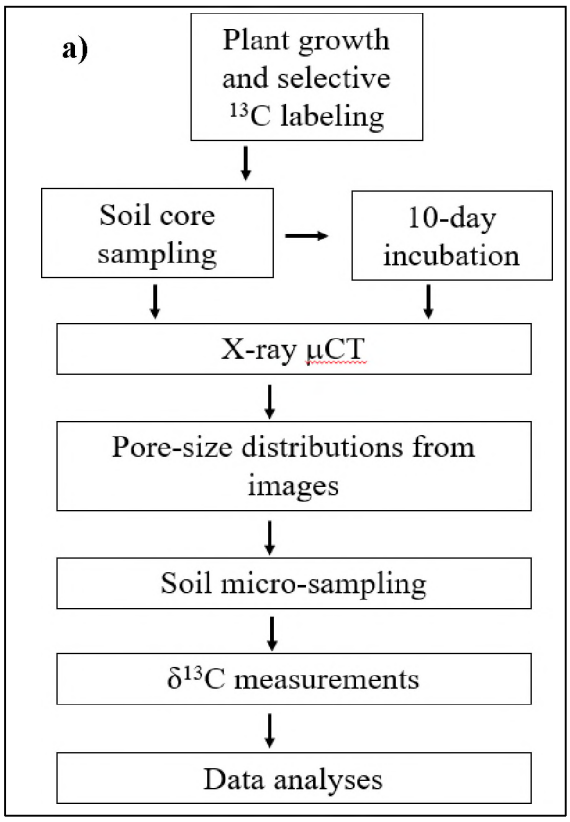

571
572
573
574
575

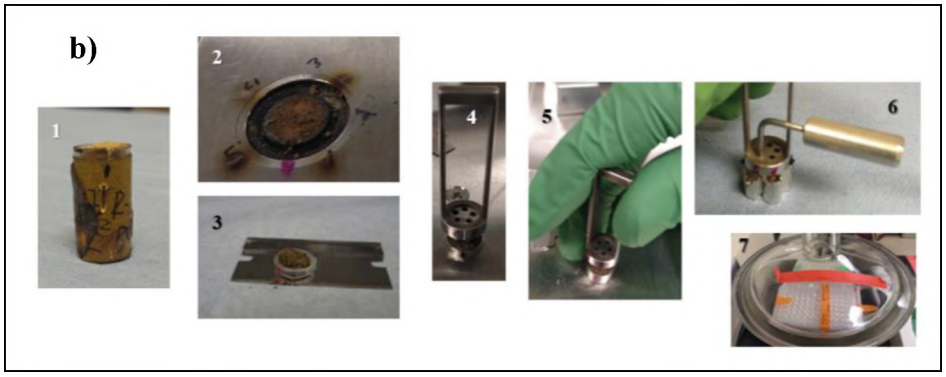

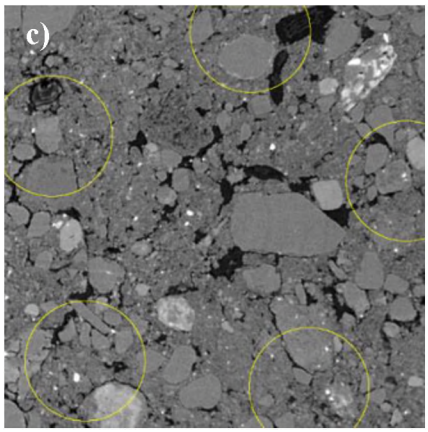

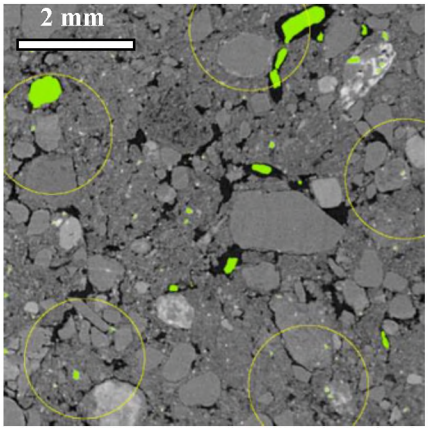

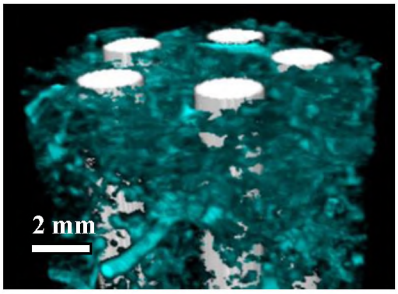

576 **Figure 2.** Soil $\delta^{13}C$ (expressed for ease of visualization as natural log of ($\delta^{13}C$ +26)) in the
577 micro-samples taken from the intact cores that were not subjected to the incubation (a) and from
578 the cores subjected to a 10-day incubation (b). Shown are the means and standard errors for the
579 means. Panels represent the C source plants, colors within each panel represent the non-labeled
580 neighbor plants. Letters mark significant differences among the non-labeled neighbors within the
581 same source (p<0.1). The red arrow line marks the system (SW-SW) that experience statistically
582 significant change in soil $\delta^{13}C$ after incubation based on all core data analyses.
583

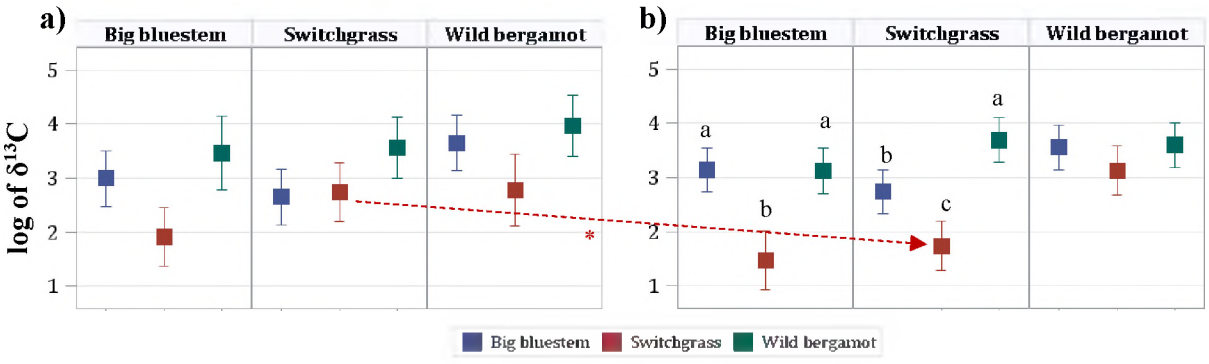

Figure 3. Difference in soil $\delta^{13}C$ between the intact non-incubated cores and post-incubation cores in all studied plant systems (a) and in plant systems grouped into those with noticeable C transfer and those without C transfer (b). The two cores (non-incubated and post-incubated) used to calculate each difference are from the same experimental pot. Positive values indicate that soil $\delta^{13}C$ in the pot decreased after the incubation. Shown on (a) are the means and standard errors for the means; panels represent the source plants, colors within each panel represent the non-labeled neighbor plants; there were no statistically significant differences among any of plant systems ($p<0.1$). Shown on (b) are the means of the differences (crosses), standard errors for the means (black lines), and individual difference data points; the difference between the plant systems with and without C transfer is statistically significant at $p<0.1$.

a)

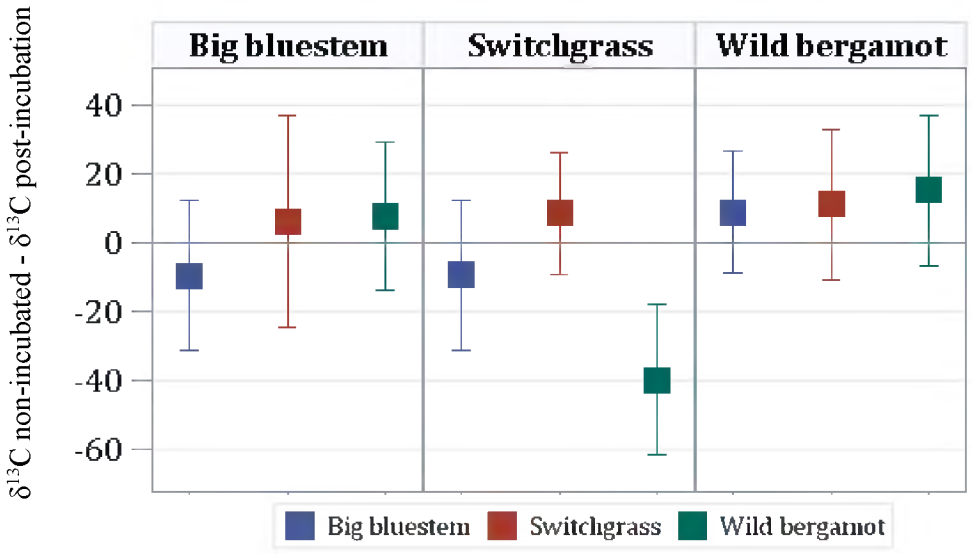

b)

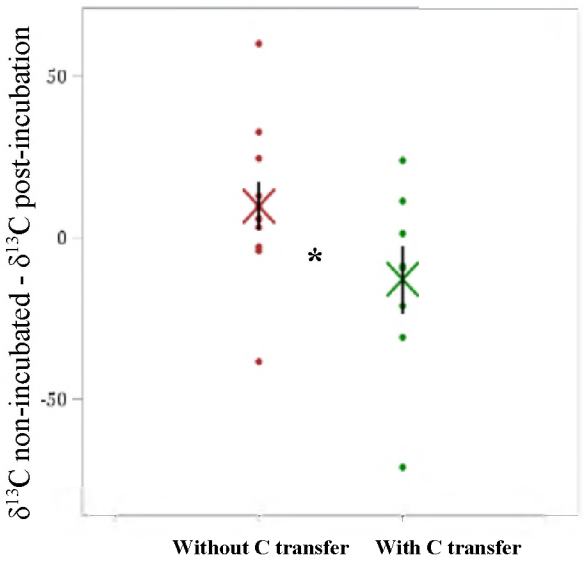

Figure 4. Examples of soil $\delta^{13}C$ signatures from micro-samples from 8 randomly selected soil cores shown at their approximate locations within the cores. Data from each core are shown with the same color.

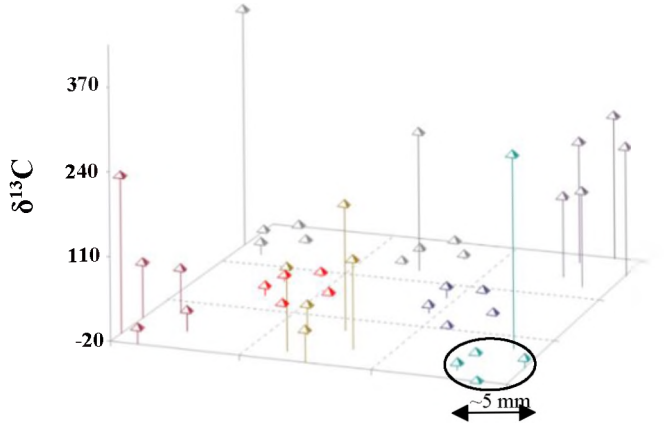

Figure 5. Pore size distributions before (yellow) and after (purple) incubation in a) the three studied plant systems shown separately for each source plant group, and b) in the systems with and without demonstrated C transfer. Grey bars mark the pore sizes within each group where there were significant differences between non- and post-incubation pore volumes, the differences are significant at $p<0.1$ on part a) and at $p<0.05$ on part b).

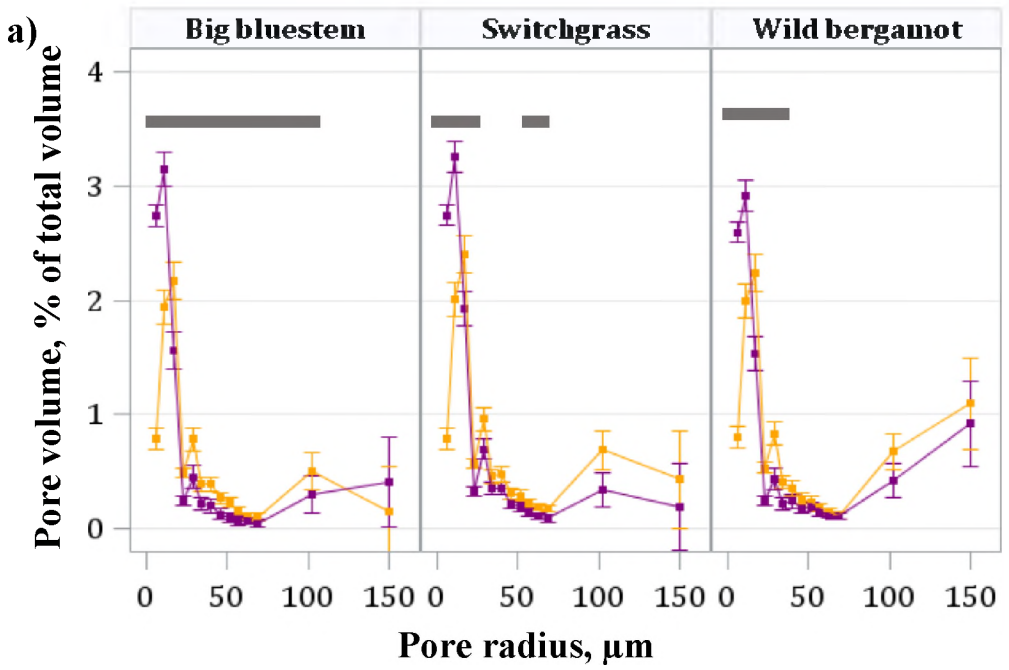

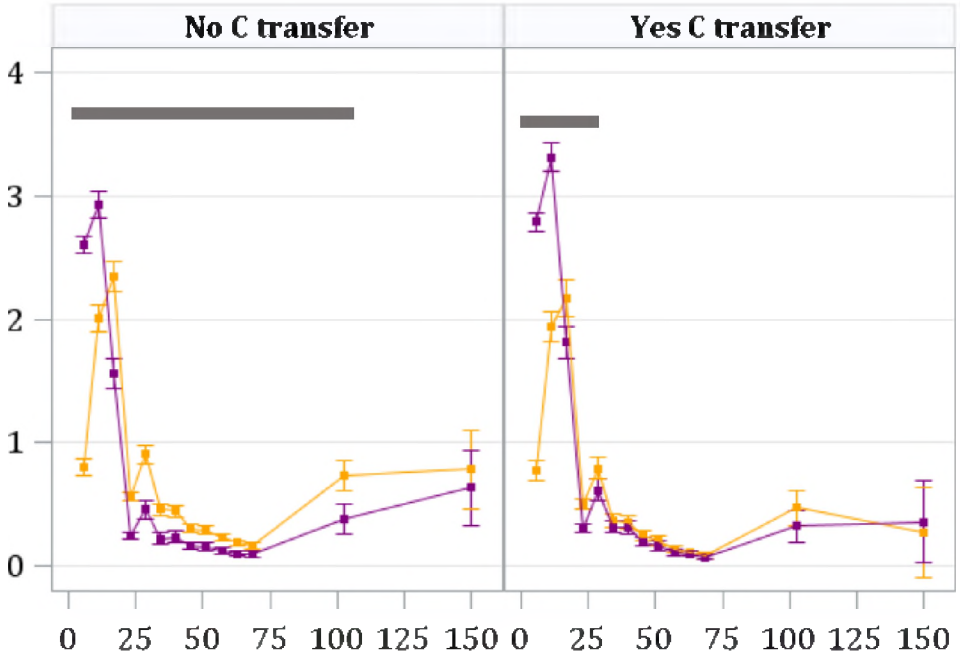

Figure 6. Correlation coefficients between plant assimilated C allocated into the soil ($\delta^{13}C$ value) and volumes of soil pores with 5.6 to 75 µm radii obtained from the non-incubated (a) and post-incubation (b) soil cores grouped by the C source plant; and from the non-incubated (c) and post-incubation (d) soil cores grouped by the C transfer group. Correlations were conducted for $\delta^{13}C$ expressed as a natural log of ($\delta^{13}C$ +26). The numbers of observations for each C source plant group are shown above the graphs. The color scale represents the values of the correlation coefficients. The correlation coefficients that are significantly different from zero are marked with ** ($p<0.05$) and * ($p<0.1$). Examples of scatter plots and regression lines for selected individual associations in non-incubated (yellow) and post-incubated (purple) cores are shown for WB (e) and SW (f). Regression coefficients significant at 0.01, 0.05, and 0.1 levels are marked with ***, **, and *, respectively.

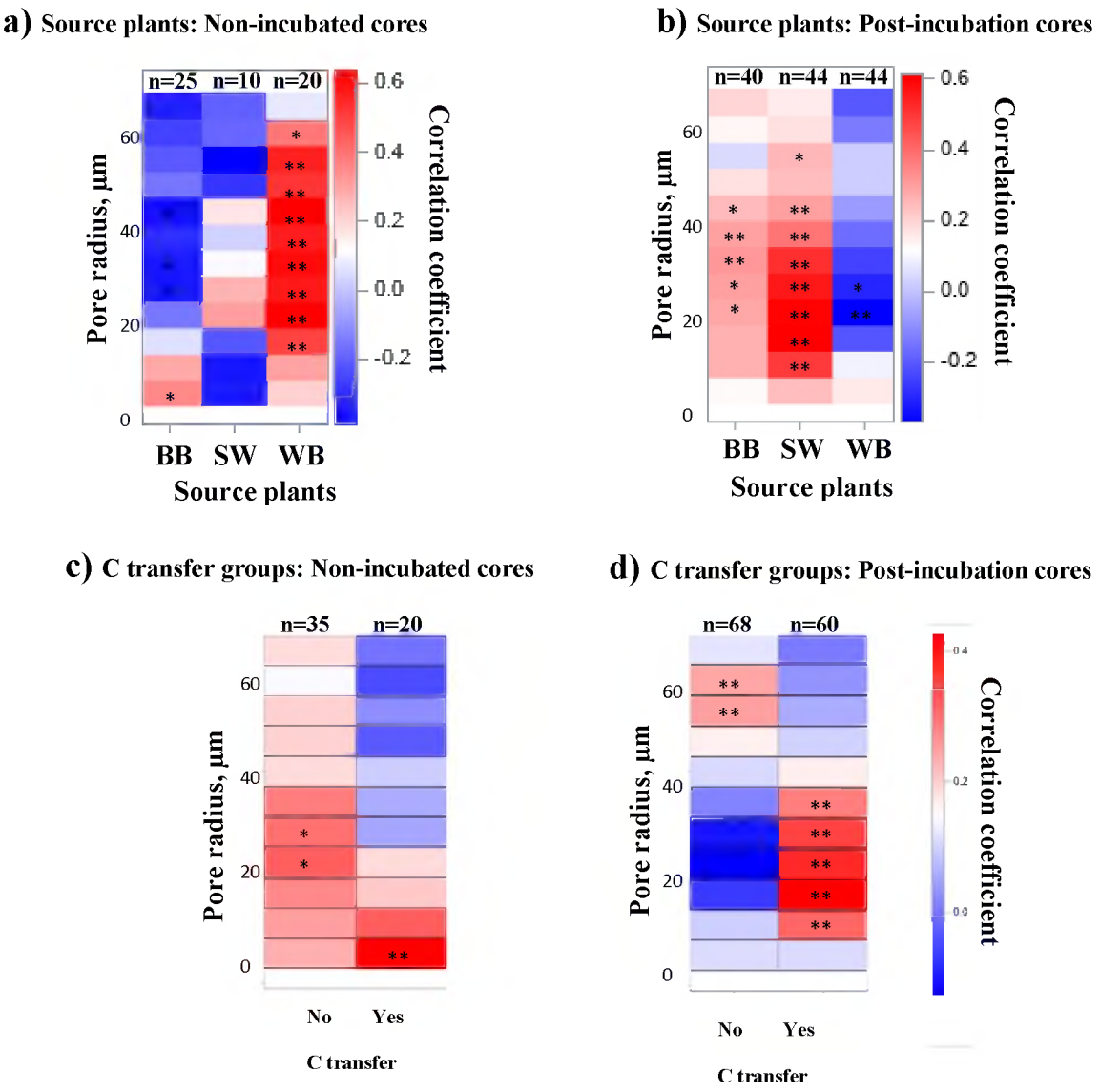

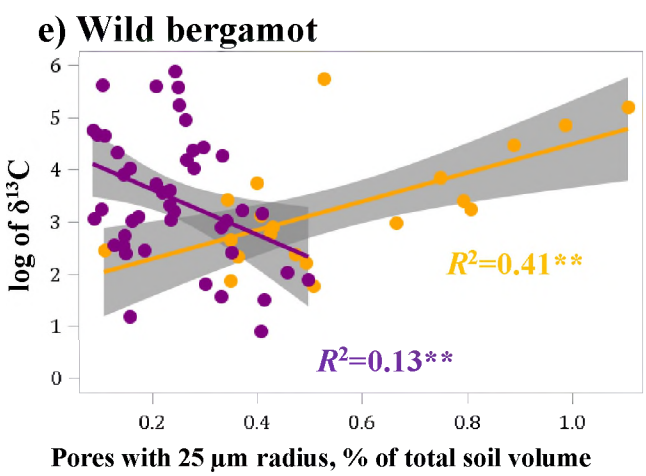
e) Wild bergamot
log of δ13C
R2=0.41**
R2=0.13**
Pores with 25 µm radius, % of total soil volume

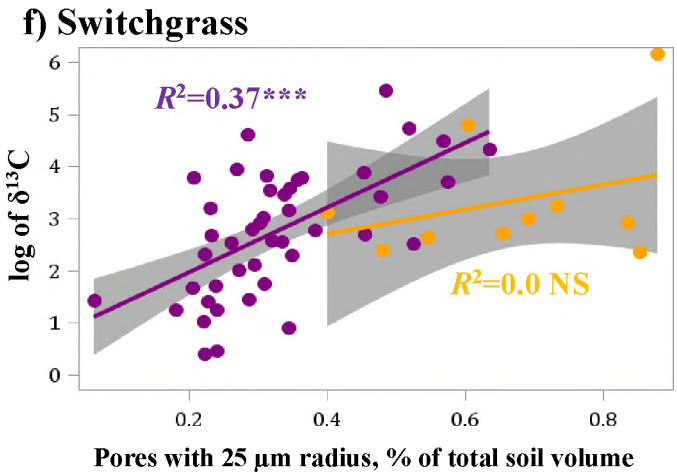
f) Switchgrass
log of δ13C
R2=0.37***
R2=0.0 NS
Pores with 25 µm radius, % of total soil volume

References

Ananyeva, K., Wang, W., Smucker, A.J.M., Rivers, M.L., Kravchenko, A.N., 2013. Can intra-aggregate pore structures affect the aggregate's effectiveness in protecting carbon? Soil Biol Biochem 57, 868-875.

Callaway, R.M., Pennings, S.C., Richards, C.L., 2003. Phenotypic plasticity and interactions among plants. Ecology 84(5), 1115-1128.

Cheng, W.X., Johnson, D.W., Fu, S.L., 2003. Rhizosphere effects on decomposition: Controls of plant species, phenology, and fertilization. Soil Sci Soc Am J 67(5), 1418-1427.

Clemmensen, K.E., Bahr, A., Ovaskainen, O., Dahlberg, A., Ekblad, A., Wallander, H., Stenlid, J., Finlay, R.D., Wardle, D.A., Lindahl, B.D., 2013. Roots and associated fungi drive long-term carbon sequestration in boreal forest. Science 339, 1615-1618.

De Deyn, G.B., Shiel, R.S., Ostle, N.J., McNamara, N.P., Oakley, S., Young, I., Freeman, C., Fenner, N., Quirk, H., Bardgett, R.D., 2011. Additional carbon sequestration benefits of grassland diversity restoration. Journal of Applied Ecology 48(3), 600-608.

De Notaris, C., Olesen, J.E., Sorensen, P., Rasmussen, J., 2020. Input and mineralization of carbon and nitrogen in soil from legume-based cover crops. Nutr Cycl Agroecosys 116(1), 1-18.

Denis, E.H., Ilhardt, P.D., Tucker, A.E., Huggett, N.L., Rosnow, J.J., Moran, J.J., 2019. Spatially tracking carbon through the root-rhizosphere-soil system using laser ablation-IRMS. Journal of Plant Nutrition and Soil Science 182(3), 401-410.

Dijkstra, F.A., Morgan, J.A., Blumenthal, D., Follett, R.F., 2010. Water limitation and plant inter-specific competition reduce rhizosphere-induced C decomposition and plant N uptake. Soil Biol Biochem 42(7), 1073-1082.

Fan, F., Zhang, F., Qu, Z., Lu, Y., 2008. Plant carbon partitioning below ground in the presence of different neighboring species. Soil Biol Biochem 40(9), 2266-2272.

Gutierrez-Castorena, M.C., Gutierrez-Castorena, E.V., Gonzalez-Vargas, T., Ortiz-Solorio, C.A., Suastegui-Mendez, E., Cajuste-Bontemps, L., Rodriguez-Mendoza, M.N., 2018. Thematic micro-maps of soil components using high-resolution spatially referenced mosaics from whole soil thin sections and image analysis. Eur J Soil Sci 69(2), 217-231.

Holz, M., Zarebanadkouki, M., Kuzyakov, Y., Pausch, J., Carminati, A., 2018. Root hairs increase rhizosphere extension and carbon input to soil. Ann Bot-London 121, 61-69.

Hupe, A., Naether, F., Haase, T., Bruns, C., Heß, J., Dyckmans, J., Joergensen, R.G., Wichern, F., 2021. Evidence of considerable C and N transfer from peas to cereals via direct root contact but not via mycorrhiza. Scientific Reports 11(1), 11424.

Hupe, A., Schulz, H., Bruns, C., Haase, T., Hess, J., Joergensen, R.G., Wichern, F., 2018. Even flow? Changes of carbon and nitrogen release from pea roots over time. Plant Soil 431(1-2), 143-157.

Johnson, D., Leake, J.R., Ostle, N., Ineson, P., Read, D.J., 2002. In situ $^{13}CO_2$ pulse-labelling of upland grassland demonstrates a rapid pathway of carbon flux from arbuscular mycorrhizal mycelia to the soil. New Phytol 153, 327-334.

Kätterer, T., Bolinder, M.A., Andrén, O., Kirchmann, H., Menichetti, L., 2011. Roots contribute more to refractory soil organic matter than above-ground crop residues, as revealed by a long-term field experiment. Agriculture, Ecosystems & Environment 141, 184-192.

Keiluweit, M., Nico, P.S., Kleber, M., Fendorf, S., 2016. Are oxygen limitations under recognized regulators of organic carbon turnover in upland soils? Biogeochemistry 127(2-3), 157-171.

Keiluweit, M., Wanzek, T., Kleber, M., Nico, P., Fendorf, S., 2017. Anaerobic microsites have an unaccounted role in soil carbon stabilization. Nat Commun 8.

Killham, K., Amato, M., Ladd, J.N., 1993. Effect of Substrate Location in Soil and Soil Pore-Water Regime on Carbon Turnover. Soil Biol Biochem 25(1), 57-62.

Koestel, J., Dathe, A., Skaggs, T.H., Klakegg, O., Ahmad, M.A., Babko, M., Giménez, D., Farkas, C., Nemes, A., Jarvis, N., 2018. Estimating the permeability of naturally structured soil from percolation theory and pore space characteristics imaged by X-ray. Water Resour Res 54(11), 9255–9263.

Kravchenko, A.N., Guber, A.K., Gunina, A., Dippold, M., Kuzyakov, Y., 2020. Pore-scale view of microbial turnover: combining 14C imaging, μCT, and zymography after adding soluble carbon to soil pores of specific sizes. Eur J Soil Sci doi.org/10.1111/ejss.13001.

Kravchenko, A.N., Guber, A.K., Rasavi, B.S., Koestel, J., Quigley, M.Y., Robertson, G.P., Kuzyakov, Y., 2019. Microbial spatial footprint as a driver of soil carbon stabilization. Nature Communications 10.

Kravchenko, A.N., Zheng, H., Kuzyakov, Y., Robertson, G.P., Guber, A.K., 2021. Belowground interplant carbon transfer promotes soil carbon gains in diverse plant communities. Soil Biology and Biochemistry.

Kuzyakov, Y., Blagodatskaya, E., 2015. Microbial hotspots and hot moments in soil: Concept & review. Soil Biol Biochem 83, 184-199.

Kuzyakov, Y., Domanski, G., 2000. Carbon input by plants into the soil. Review. Journal of Plant Nutrition and Soil Science 163(4), 421-431.

Kuzyakov, Y., Razavi, B.S., 2019. Rhizosphere size and shape: Temporal dynamics and spatial stationarity. Soil Biol Biochem 135, 343-360.

Ladygina, N., Hedlund, K., 2010. Plant species influence microbial diversity and carbon allocation in the rhizosphere. Soil Biol Biochem 42(2), 162-168.

Lucas, M., Pihlap, E., Steffens, M., Vetterlein, D., Koegel-Knabner, I., 2020. Combination of Imaging Infrared Spectroscopy and X-ray Computed Microtomography for the Investigation of Bio- and Physicochemical Processes in Structured Soils. Frontiers in Environmental Science 8.

Marx, M., Buegger, F., Gattinger, A., Zsolnay, A., Munch, J.C., 2007. Determination of the fate of C-13 labelled maize and wheat exudates in an agricultural soil during a short-term incubation. Eur J Soil Sci 58(5), 1175-1185.

Montesinos-Navarro, A., Verdu, M., Ignacio Querejeta, J., Valiente-Banuet, A., 2017. Nurse plants transfer more nitrogen to distantly related species. Ecology 98(5), 1300-1310.

Mortensen, E.O., De Notaris, C., Peixoto, L., Olesen, J.E., Rasmussen, J., 2021. Short-term cover crop carbon inputs to soil as affected by long-term cropping system management and soil fertility. Agriculture Ecosystems & Environment 311.

Mueller, C.W., Weber, P.K., Kilburn, M.R., Hoeschen, C., Kleber, M., Pett-Ridge, J., 2013. Advances in the Analysisof Biogeochemical Interfaces: NanoSIMS to Investigate Soil Microenvironments. Advances in Agronomy 121, 1-46.

Munch, B., Holzer, L., 2008. Contradicting geometrical concepts in pore size analysis attained with electron microscopy and mercury intrusion. J Am Ceram Soc 91(12), 4059-4067.

Negassa, W., Guber, A.K., Kravchenko, A.N., Marsh, T.L., Hildebrandt, B., Rivers, M.L., 2015. Properties of soil pore space regulate pathways of plant residue decomposition and community structure of associated bacteria. Plos One.

Nunan, N., Ritz, K., Rivers, M., Feeney, D.S., Young, I.M., 2006. Investigating microbial micro-habitat structure using X-ray computed tomography. Geoderma 133(3-4), 398-407.

Nunan, N., Wu, K.J., Young, I.M., Crawford, J.W., Ritz, K., 2003. Spatial distribution of bacterial communities and their relationships with the micro-architecture of soil. Fems Microbiol Ecol 44(2), 203-215.

Pagel, H., Kriesche, B., Uksa, M., Poll, C., Kandeler, E., Schmidt, V., Streck, T., 2020. Spatial Control of Carbon Dynamics in Soil by Microbial Decomposer Communities. Frontiers in Environmental Science 8(2).

Pausch, J., Kuzyakov, Y., 2011. Photoassimilate allocation and dynamics of hotspots in roots visualized by C-14 phosphor imaging. Journal of Plant Nutrition and Soil Science 174(1), 12-19.

749 Pausch, J., Kuzyakov, Y., 2017. Carbon input by roots into the soil: quantification of rhizodeposition from
750 root to ecosystem scale. Global Change Biol 24, 1-12.
751 Pausch, J., Kuzyakov, Y., 2018. Carbon input by roots into the soil: Quantification of rhizodeposition from
752 root to ecosystem scale. Global Change Biol 24(1), 1-12.
753 Pausch, J., Zhu, B., Kuzyakov, Y., Cheng, W., 2013. Plant inter-species effects on rhizosphere priming of
754 soil organic matter decomposition. Soil Biol Biochem 57, 91-99.
755 Peixoto, L., Elsgaard, L., Rasmussen, J., Kuzyakov, Y., Banfield, C.C., Dippold, M.A., Olesen, J.E., 2020.
756 Decreased rhizodeposition, but increased microbial carbon stabilization with soil depth down to
757 3.6 m. Soil Biol Biochem 150.
758 Pfeffer, P.E., Douds, D.D., Bucking, H., Schwartz, D.P., Shachar-Hill, Y., 2004. The fungus does not
759 transfer carbon to or between roots in an arbuscular mycorrhizal symbiosis. New Phytol 163(3),
760 617-627.
761 Portell, X., Pot, V., Garnier, P., Otten, W., Baveye, P.C., 2018. Microscale heterogeneity of the spatial
762 distribution of organic matter can promote bacterial biodiversity in soils: insights from computer
763 simulations. Front Microbiol 9, 1583.
764 Quigley, M.Y., Negassa, W.C., Guber, A.K., Rivers, M.L., Kravchenko, A.N., 2018. Influence of pore
765 characteristics on the fate and distribution of newly added carbon Frontiers in Environmental
766 Science 13.
767 Rasband, W.S., 1997-2015. ImageJ. U.S. National Institutes of Health, Bethesda, MD, USA. .
768 Rasmussen, J., Eriksen, J., Jensen, E.S., Esbensen, K.H., Hogh-Jensen, H., 2007. In situ carbon and
769 nitrogen dynamics in ryegrass-clover mixtures: Transfers, deposition and leaching. Soil Biol
770 Biochem 39(3), 804-815.
771 Robinson, D., Fitter, A., 1999. The magnitude and control of carbon transfer between plants linked by a
772 common mycorrhizal network. J Exp Bot 50(330), 9-13.
773 Ruamps, L.S., Nunan, N., Chenu, C., 2011. Microbial biogeography at the soil pore scale. Soil Biol
774 Biochem 43(2), 280-286.
775 Ruamps, L.S., Nunan, N., Pouteau, V., Leloup, J., Raynaud, X., Roy, V., Chenu, C., 2013. Regulation of soil
776 organic C mineralisation at the pore scale. Fems Microbiol Ecol 86(1), 26-35.
777 Sanaullah, M., Blagodatskaya, E., Chabbi, A., Rumpel, C., Kuzyakov, Y., 2011. Drought effects on
778 microbial biomass and enzyme activities in the rhizosphere of grasses depend on plant
779 community composition. Appl Soil Ecol 48(1), 38-44.
780 Sanaullah, M., Chabbi, A., Rumpel, C., Kuzyakov, Y., 2012. Carbon allocation in grassland communities
781 under drought stress followed by C-14 pulse labeling. Soil Biol Biochem 55, 132-139.
782 Schindelin, J., Arganda-Carreras, I., Frise, E., Kaynig, V., Longair, M., Pietzsch, T., Preibisch, S., Rueden, C.,
783 Saalfeld, S., Schmid, B., Tinevez, J.Y., White, D.J., Hartenstein, V., Eliceiri, K., Tomancak, P.,
784 Cardona, A., 2012. Fiji: an open-source platform for biological-image analysis. Nat Methods 9(7),
785 676-682.
786 Simard, S.W., Beiler, K.J., Bingham, M.A., Deslippe, J.R., Philip, L.J., Teste, F.P., 2012. Mycorrhizal
787 networks: Mechanisms, ecology and modelling. Fungal Biology Reviews 26(1, Sp. Iss. SI), 39-60.
788 Simard, S.W., Perry, D.A., Jones, M.D., Myrold, D.D., Durall, D.M., Molina, R., 1997. Net transfer of
789 carbon between ectomycorrhizal tree species in the field. Nature 388(6642), 579-582.
790 Smith, S.E., Smith, F.A., 2011. Roles of arbuscular mycorrhizas in plant nutrition and growth: new
791 paradigms from cellular to ecosystem scales. In: S.S. Merchant, W.R. Briggs, D. Ort (Eds.), Annual
792 Review of Plant Biology. Annual Review of Plant Biology, pp. 227-250.
793 Sprunger, C.D., Robertson, G.P., 2018. Early accumulation of active fraction soil carbon in newly
794 established cellulosic biofuel systems. Geoderma 318, 42-51.
795 Sterner, R.W., Elser, J.J., 2002. Ecological Stochiometry: The Biology of Elements from Molecules to the
796 Biosphere. Princeton Univ. Press.

Strong, D.T., De Wever, H., Merckx, R., Recous, S., 2004. Spatial location of carbon decomposition in the soil pore system. Eur J Soil Sci 55(4), 739-750.

Vidal, A., Hirte, J., Bender, S.F., Mayer, J., Gattinger, A., Hoeschen, C., Schaedler, S., Iqbal, T.M., Mueller, C.W., 2018. Linking 3D Soil Structure and Plant-Microbe-Soil Carbon Transfer in the Rhizosphere. Frontiers in Environmental Science 6.

Vogel, H.J., Weller, U., Schluter, S., 2010. Quantification of soil structure based on Minkowski functions. Comput Geosci-Uk 36(10), 1236-1245.

Warembourg, F.R., Roumet, C., Lafont, F., 2004. Interspecific control of non-symbiotic carbon partitioning in the rhizosphere of a grass-clover association: Bromus madritensis-Trifolium angustifolium. J Exp Bot 55(397), 743-750.

Wichern, F., Mayer, J., Joergensen, R.G., Mueller, T., 2007a. Release of C and N from roots of peas and oats and their availability to soil microorganisms. Soil Biol Biochem 39(11), 2829-2839.

Wichern, F., Mayer, J., Joergensen, R.G., Mueller, T., 2007b. Rhizodeposition of C and N in peas and oats after C-13-N-15 double labelling under field conditions. Soil Biol Biochem 39(10), 2527-2537.

Appendix

Appendix Fig.1. An X-ray computed tomography scan of one of the studied pots at the end of the incubation showing plant roots and soil fragments with the same range of grayscale values as the roots.

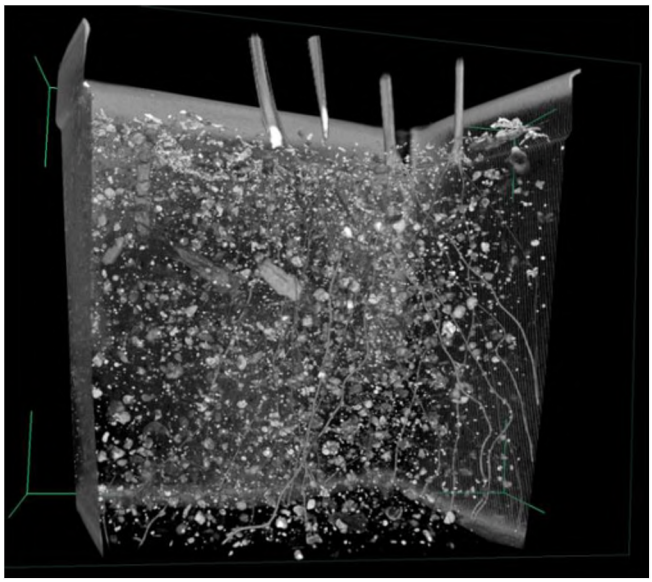

Appendix Fig.2. Schematic representation of soil core collection.

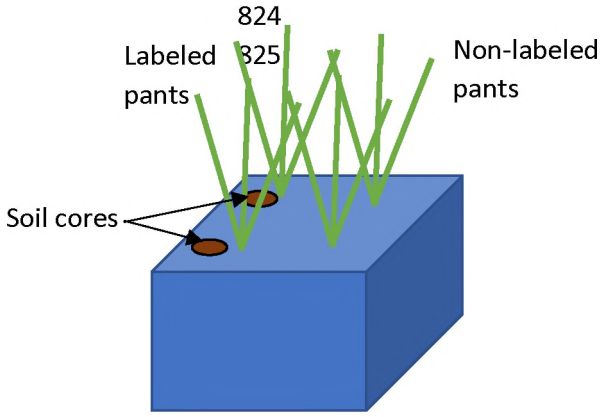

826 **Appendix Fig. 3.** Soil $\delta^{13}C$ grouped by the presence of the interplant C transfer plotted vs.
827 volumes of plant roots (a) and particulate organic matter fragments (b) identified using X-ray
828 µCT images within each soil micro-sample.

829

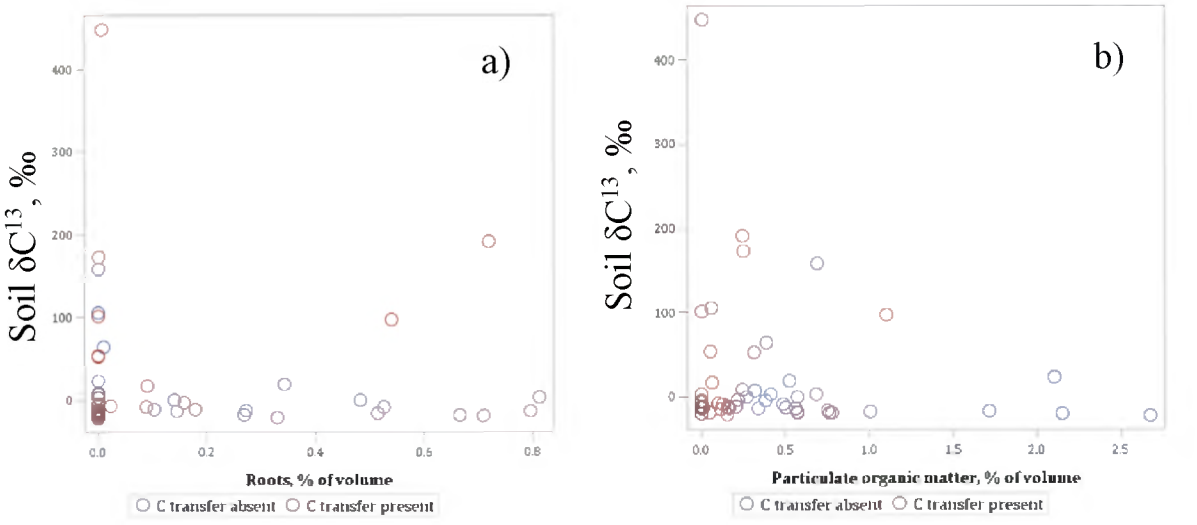

Appendix Fig.4. Soil $\delta^{13}C$ (expressed for ease of visualization as natural log of ($\delta^{13}C$ +26)) grouped by the presence and absence of C transfer with wild bergamot (WB) C source data as a separate group, and grasses switchgrass (SW) and big bluestem (BB) presented separately in the systems with C transfer (Yes) and without C transfer (No).